Please cite this article in press as: Floquet et al., Conformational Equilibrium of CDK/Cyclin Complexes by Molecular Dynamics with Excited Normal Modes, Biophysical Journal (2015), http://dx.doi.org/10.1016/j.bpj.2015.07.003

Article

Conformational Equilibrium of CDK/Cyclin Complexes by Molecular Dynamics with Excited Normal Modes

Nicolas Floquet,[1,*] Mauricio G. S. Costa,[2] Paulo R. Batista,[2] Pedro Renault,[3] Paulo M. Bisch,[3] Florent Raussin,[1] Jean Martinez,[1] May C. Morris,[1] and David Perahia[4,*]

[1]Institut des Biomolécules Max Mousseron (IBMM), Centre National de la Recherche Scientifique UMR 5247, Université de Montpellier, Ecole Normale Supérieure de Chimie de Montpellier, Faculté de Pharmacie, Montpellier, France; [2]Programa de Computação Científica, Fundação Oswaldo Cruz, Rio de Janeiro, Brazil; [3]Instituto de Biofísica Carlos Chagas Filho, Universidade Federal do Rio de Janeiro, Rio de Janeiro, Brazil; and [4]Laboratoire de Biologie et de Pharmacologie Appliquée, Ecole Normale Supérieure de Cachan, Centre National de la Recherche Scientifique, Cachan, France

ABSTRACT Cyclin-dependent kinases (CDKs) and their associated regulatory cyclins are central for timely regulation of cell-cycle progression. They constitute attractive pharmacological targets for development of anticancer therapeutics, since they are frequently deregulated in human cancers and contribute to sustained, uncontrolled tumor proliferation. Characterization of their structural/dynamic features is essential to gain in-depth insight into structure-activity relationships. In addition, the identification of druggable pockets or key intermediate conformations yields potential targets for the development of novel classes of inhibitors. Structural studies of CDK2/cyclin A have provided a wealth of information concerning monomeric/heterodimeric forms of this kinase. There is, however, much less structural information for other CDK/cyclin complexes, including CDK4/cyclin D1, which displays an alternative (open) position of the cyclin partner relative to CDK, contrasting with the closed CDK2/cyclin A conformation. In this study, we carried out normal-mode analysis and enhanced sampling simulations with our recently developed method, molecular dynamics with excited normal modes, to understand the conformational equilibrium on these complexes. Interestingly, the lowest-frequency normal mode computed for each complex described the transition between the open and closed conformations. Exploration of these motions with an explicit-solvent representation using molecular dynamics with excited normal modes confirmed that the closed conformation is the most stable for the CDK2/cyclin A complex, in agreement with their experimentally available structures. On the other hand, we clearly show that an open↔closed equilibrium may exist in CDK4/cyclin D1, with closed conformations resembling that captured for CDK2/cyclin A. Such conformational preferences may result from the distinct distributions of frustrated contacts in each complex. Using the same approach, the putative roles of the Thr^{160} phosphoryl group and the T-loop conformation were investigated. These results provide a dynamic view of CDKs revealing intermediate conformations not yet characterized for CDK members other than CDK2, which will be useful for the design of inhibitors targeting critical conformational transitions.

INTRODUCTION

Cyclin-dependent kinases (CDKs) are serine/threonine proline-directed kinases, which are inactive in their monomeric form but upon association to a family of regulatory subunits, cyclins, form functional heterodimeric complexes (1,2). To date, 20 different CDKs have been reported in mammalian cells and about the same number of cyclins (3). Although CDK1, CDK2, CDK4, and CDK6 are recognized regulators of cell-cycle progression (4), other CDKs are implicated in non-cell-cycle, unrelated biological pathways (5). Several members of this family of kinases frequently have been described as deregulated in human cancers (6). CDK/cyclins are therefore now fully recognized as pharmacological targets of interest for the development of anticancer therapeutics (7–9). Although CDKs are constantly expressed throughout the cell cycle, their cyclin partners are periodically expressed and degraded according to specific spatio-temporal patterns in healthy cells, thus dictating formation and subsequent activation of their kinase partners in a sequential and orderly fashion (1).

The general structure of CDKs is conserved throughout the protein family, with a typical bilobal fold harboring a conserved ATP-binding pocket within the N-terminal lobe. The catalytic cleft of CDKs is located at the interface of the two lobes. Likewise, cyclins are characterized by a compact α-helix-rich cyclin fold, with variations in the length and relative position of the helices. The nature of surface residues can vary significantly in both CDKs and cyclins, further defining substrate and partner specificities (10). Indeed, the cyclin partner directly contributes to substrate recruitment through specific docking sites (11).

Activation of CDK/cyclin complexes is further subject to several levels of control through reversible phosphorylations as well as through interactions with structural inhibitors. A first level of control occurs through phosphorylation of

Submitted March 2, 2015, and accepted for publication July 1, 2015.

*Correspondence: nicolas.floquet@univ-montp1.fr or david.perahia@ens-cachan.fr

Nicolas Floquet and Mauricio G. S. Costa contributed equally to this work.

Editor: Ozlem Keskin.

0006-3495/15/09/0001/11

http://dx.doi.org/10.1016/j.bpj.2015.07.003

Please cite this article in press as: Floquet et al., Conformational Equilibrium of CDK/Cyclin Complexes by Molecular Dynamics with Excited Normal Modes, Biophysical Journal (2015), http://dx.doi.org/10.1016/j.bpj.2015.07.003

residues that line the nucleotide-binding pocket, thus preventing ATP binding (12). In contrast, phosphorylation of the kinase T-loop by the CDK-activating kinase CAK (on Thr^{160} for CDK2) contributes to CDK activation (13). Many x-ray structures are available for the archetypal CDK2, describing this kinase in its monomeric form or in complex with its main partner, cyclin A.

The primary interaction between CDKs and cyclins involves the conserved αC-helix (the PSTAIRE helix in CDK2) and α-helix 5 of the cyclin (see Fig. 1) (14). Cyclin binding to a CDK induces conformational changes in the kinase subunit, as highlighted in the available crystal structures of CDK2/cyclin A and further evidenced through mechanistic and kinetic studies (14,15). Specifically, comparison between the structures of monomeric CDK2 and CDK2/cyclin A shows that cyclin binding induces a reorientation of the ATP-binding pocket, leading to its alignment with the catalytic cleft. Moreover, the presence of cyclin A is associated with a conformational switch of the activation segment (or T-loop) of CDK2, thereby rendering the substrate binding cleft more accessible and exposing this loop for further phosphorylation. In this configuration, the surface of interaction between the CDK2 and cyclin A is important, and the heterodimeric complex can be considered in a closed conformation (see Fig. 1). Phosphorylation of CDK2 on Thr^{160} stabilizes the position of the T-loop, thus favoring substrate binding, which ultimately leads to an improved catalysis of the phosphotransfer reaction (13,16,17).

Other CDK/cyclin complexes are much less represented in the Protein Data Bank (PDB). However, solved structures for the CDK4/cyclin D1 (PDB 2W9F) (18), CDK4/cyclin D3 (PDB 3G33) (19) and CDK6/cyclin K (PDB 1G3N) (20) complexes reveal a different orientation of the cyclin relative to the CDK, which will be termed as the open conformation hereafter. This conformation is most often associated with an inactive raised state of the T-loop (see Fig. 1). The CDK9/cyclin T1 complex (PDB 3BLH) (21) makes an exception, however, harboring the T-loop in an active conformation but with the cyclin partner in the open position (see Fig. 1). In this open conformation, the interface between the CDK and the cyclin is essentially provided by the αC-helix. The rotation induced upon cyclin binding is a critical step in CDK/cyclin activation, since it aligns the ATP-binding pocket in the N-terminal lobe of the CDK with the substrate binding cleft (14)

After structural alignment of the kinase fold of two representative CDK/cyclin complexes, one in a closed and one in an open conformation (CDK2/cyclin A and CDK4/cyclin D1, respectively), the resulting root-mean-square deviation (RMSD) computed on the cyclin partner is ~23 Å, which suggests that the two complexes have different modes of regulation (18). In this study, we argued whether such a large conformational rearrangement would be energetically favorable and whether it is representative of all CDK/cyclin complexes.

Normal mode analysis (NMA) is an efficient method for identifying such large-amplitude motions that could hardly

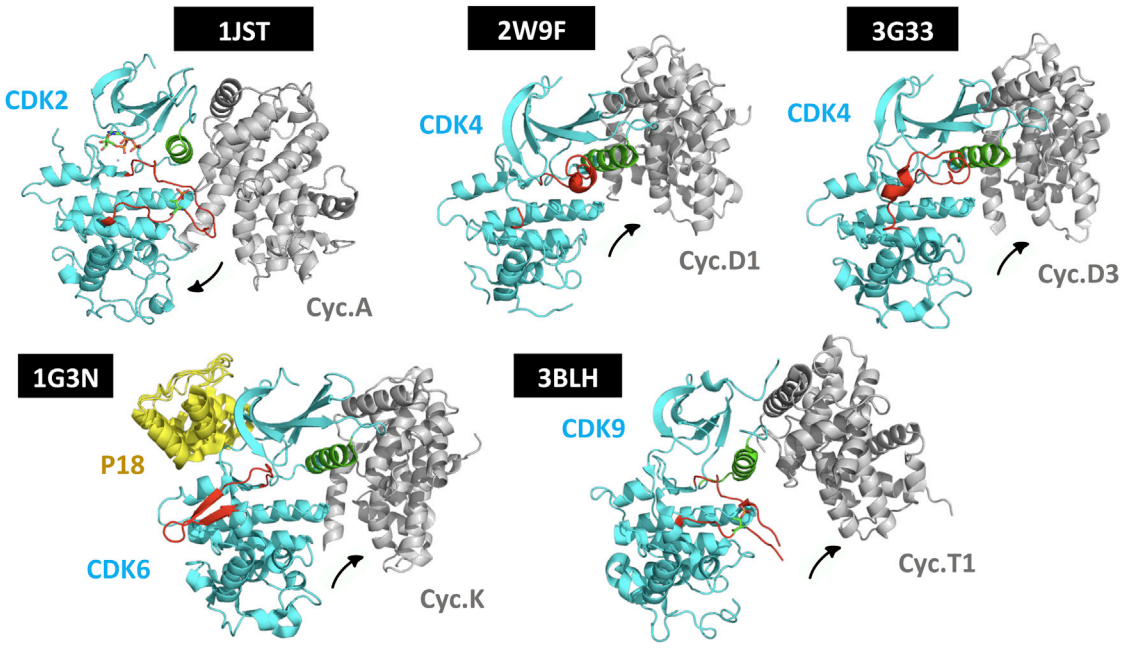

FIGURE 1 Representative closed (1JST) and open (2W9F, 3G33, 1G3N, and 3BLH) structures of CDK/cyclin complexes available in the PDB. In each complex, the kinase and cyclin subunits are reported in cyan and light gray, respectively. The αC-helix and the T-loop are highlighted in green and red, respectively. In the CDK2/cyclin A complex (PDB 1JST), the ATP and the phosphoryl group on Thr^{160} are reported in colored sticks. Furthermore, calculations in this study were performed on both the 1JST and 2W9F structures. To see this figure in color, go online.

Please cite this article in press as: Floquet et al., Conformational Equilibrium of CDK/Cyclin Complexes by Molecular Dynamics with Excited Normal Modes, Biophysical Journal (2015), http://dx.doi.org/10.1016/j.bpj.2015.07.003

be explored by classical molecular dynamics (MD) simulations (22). From NMA, the eigenvectors corresponding to the lowest frequencies are associated to the most collective motions of the protein, and are generally involved in its function (23). We have previously shown that although normal modes (NMs) are calculated in vacuum, these directions can successfully describe conformational transitions in proteins, showing remarkable agreement with structural observations (24–26). However, the major drawback of NMA resides in the fact that it neglects the structural and energetical effects of the surrounding water molecules, thus impairing proper estimation of the amplitude of the modes. Recently, we proposed MD with excited NMs (MDeNM) (27) as an alternative method that uses the low-frequency NMs computed in vacuum as privileged directions in MD simulations with an explicit representation of the surrounding medium. In addition, we applied this method to simulate large protein/protein complexes in a membrane model (28).

In this study, the NMs of the CDK2/cyclin A and CDK4/cyclin D1 complexes were computed to identify the intrinsic large-amplitude motions of CDK/cyclin complexes. After identification of modes that successfully described the expected conformational transition, the MDeNM approach was used to explore the equilibrium populations of conformers related to this motion in each complex, taking into account the full aqueous environment.

MATERIALS AND METHODS

Initial structures/models

In this study, two different x-ray structures available in the PDB were considered: 1) the 1JST structure (17), describing the CDK2/cyclin A complex, with a bound ATP, a phosphorylated Thr^{160}, and an active T-loop conformation; and 2) the 2W9F structure (18), corresponding to the CDK4/cyclin D1 complex, with an inactive T-loop conformation (see Fig. 1).

Calculations were also performed on the 1JST structure after removal of the phosphorylation group on Thr^{160} (1JST_NOP), and on a 2W9F-based model in which the activation loop was artificially introduced in an active conformation by homology with 1JST (2W9F_HYBRID). The latter was modeled using Modeler software (29). The best model according to the internal score of the software was selected among the 50 produced models for further calculations. The entire homology modeling procedure was performed considering the presence of the cyclin D1 partner.

MD and NMA

Each starting structure (1JST, 1JST_NOP, 2W9F, and 2W9F_HYBRID) was built using the CHARMM program (version 36) (30,31) with force-field parameter set 27 and was inserted in a cubic box of TIP3 water molecules, leaving at least 15 Å of water-shell thickness on all sides of the protein/protein complex. Ions were added so that the global charge of each system was neutralized. After a short energy minimization combining steepest descent and adopted-basis Newton Raphson algorithms, a 500 ps equilibration dynamics of the system was performed with CHARMM using the Nosé-Hoover algorithm with the temperature fixed at 300 K (NVT conditions) and an integration step of 1 fs. During these calculations, positional restraints were applied only to the backbone atoms of the protein. Electrostatic interactions were computed using a cutoff value of 12 Å and the particle-mesh Ewald method. The final equilibrated structure from the MD simulations was considered for NMA. This structure was energy minimized in vacuum using a cutoff value of 10 Å but with a switching function applied between 10 and 12 Å. A distance-dependent dielectric constant of $2r$ was used, where r is the interatomic distance. After minimization in vacuum, the 50 lowest-frequency NMs were computed using the DIMB module of CHARMM (32).

The VMOD module as implemented in CHARMM was further used, as we described previously, to generate energy-minimized conformations in vacuum along the directions corresponding to each of the first 10 lowest-frequency NMs. Briefly explained, this approach consists of displacements along NM coordinates while performing energy minimizations, with harmonic restraints at different windows. For more details, please refer to Floquet et al. (24). In this study, a mass-weighted root mean-square (MRMS) step of 0.2 Å was used to generate conformations in the range from −6 to 6 Å along each of the NM vectors considered. These models were used to identify the mode(s) of interest, e.g., those that describe the transition between the open and closed conformations of CDK/cyclin complexes.

Exploration of NMs with explicit representation of the solvent

The mode(s) of interest corresponding to the open/closed conformational transition were then used to perform MDeNM simulations with explicit representation of the solvent (27). The velocities of all the atoms of the system were reread from the ending point of the 500 ps equilibration trajectory. Using the same force-field parameters, and without any applied restraint, 40 MDeNM replicas were performed for each simulated system. Each excitation consists of assigning the considered NM as an incremental velocity added to those obtained from the last frame of equilibration (for the first excitation) or from the previous MDeNM simulation (for subsequent excitations). These additional velocities define the excitation temperature that is added to the current temperature promoting a motion along the positive or negative direction along the mode.

Because of the rapid dissipation of this excitation energy due to atomic motions along other degrees of freedom and to the constant temperature algorithm, the MDeNM simulations were performed under periodic excitations (in this case, five). Each replica corresponds to a random value of the excitation temperature and a random direction for the excitation (positive or negative) along the mode. After this step, 4000 conformers (40 replicas × 5 excitations × 20 ps) obtained for each system were grouped, and the Carma software (33) was used to compute a Cα-Cα RMSD matrix of the concatenated trajectory so obtained. This full set of conformations was then reduced to its 20 most representative members using the k-means algorithm implemented in the R software (www.r-project.org). After the clustering procedure, an additional 2 ns of unrestrained MD simulations was carried out starting from each of the 20 clusters, using NAMD (34) and the same force-field parameters that were used with CHARMM. This conformational exploration step yielded a final 40 ns concatenated trajectory. All resulting conformations of this trajectory were projected on the chosen NM vector for further amplitude/population analyses. The projections correspond to the scalar product between the atomic displacement vector (the difference between the displaced conformation and the initial conformation from which the NMs were computed) and the NM vector. Since the NM vector is a mass-weighted unit vector, the atomic displacement vector was mass weighted before the projection. Thus, each component of the displacement vector was multiplied by $\sqrt{m_i/M}$ (24). For a pure displacement vector (which coincides with the NM vector), the square of the projection corresponds to the MRMS difference between the displaced and the initial structures. Thus, for a given structural displacement arising from an MD simulation, the real MRMS values with respect to the initial structure (referred to here as the RMSD) are larger than the MRMS values obtained by the projections onto the NM vector (see Fig. 3). The protocol used in this study is summarized in Fig. 2.

Please cite this article in press as: Floquet et al., Conformational Equilibrium of CDK/Cyclin Complexes by Molecular Dynamics with Excited Normal Modes, Biophysical Journal (2015), http://dx.doi.org/10.1016/j.bpj.2015.07.003

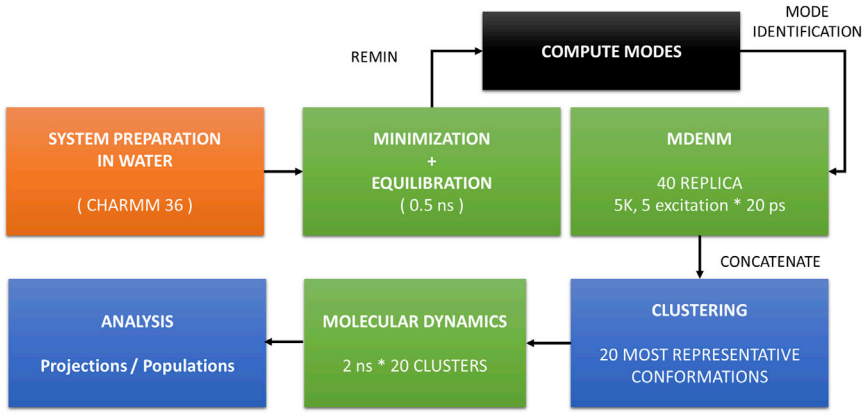

FIGURE 2 Summary of the protocol used in this study for the CDK2/cyclin A (1JST), CDK4/cyclin D1 (2W9F), 1JST_NOP, and 2W9F_HYBRID complexes. To see this figure in color, go online.

Analysis of experimental structural variations

Experimental conformations were obtained using ProDy v.1.5.1 (35). First, a blast search against the PDB database was performed to retrieve structures sharing at least 70% sequence identity with the reference complex (CDK2/cyclin A or CDK4/cyclin D1). Then, the obtained ensembles were superimposed using the Kabsch algorithm as described in Bakan and Bahar (36). Only Cα atoms were considered in these calculations. A principal-component analysis (PCA) was then performed to identify the most relevant structural variations of the experimental data set. A list of the PDB IDs of this experimental data set is provided in the Supporting Material. The PCA procedure is based on the diagonalization of the covariance matrix, $\boldsymbol{c}$, of atomic positions whose elements are represented by

$$c_{(i,j)} = \langle \Delta r_i \cdot \Delta r_j \rangle,$$

where Δr_i and Δr_j indicate the displacement vectors of atoms i and j, respectively, from their average positions. Brackets stand for ensemble averages. Then, an eigenvalue problem is solved, resulting in $3N$ PCs, which can be sorted according to their fractional contributions to the overall variance.

Dynamical cross-correlation analysis

Correlation coefficients between pairs of residues were calculated from the covariance matrix of atomic positions ($c_{(i,j)}$) considering only the positions of Cα atoms. The cross-correlation matrices, C (normalized covariance), were calculated according to the equation

$$C_{(i,j)} = \frac{\langle \Delta r_i \cdot \Delta r_j \rangle}{\langle \Delta r_i^2 \rangle^{1/2} \cdot \langle \Delta r_j^2 \rangle^{1/2}}.$$

In the above equation, fully correlated motions have a value of $+1$ and completely anticorrelated motions have a value of -1. This analysis was intended to identify correlated regions within a given protein. Calculations were conducted with R software using the Bio3D package (37).

Local frustration analysis

All energetic frustration analyses were conducted with the Frustratometer web server (38). Calculations were performed considering CDK/cyclin complexes in both open and closed states. The CDK-2/cyclin A open state and CDK-4/cyclin D1 closed state were obtained upon 4 Å displacements along their corresponding lowest-frequency modes. Briefly, the program calculates the energetic frustration of each contact on the structure submitted by the user in comparison to a set of generated decoy states where the identities of each residue are mutated. A contact is defined as minimally frustrated or highly frustrated by comparing its frustration energy with the values obtained from the decoy states, as further described in Ferreiro et al. (39).

RESULTS

The lowest-frequency mode of CDK/cyclin complexes describes an open/closed conformational transition

After preparation and energy minimizations (with CHARMM) of the two CDK2/cyclin A (PDB 1JST, closed conformation) and CDK4/cyclin D1 (PDB 2W9F, open conformation) complexes, their 50 lowest-frequency NMs were computed. Subsequently, the VMOD subroutine was applied to generate 61 energy-minimized conformations along each of the first 10 lowest-frequency NMs for each complex. In both cases, the lowest-frequency motion accounted for ~40–50% of the overall dynamics, whereas the cumulative contribution of the first five modes was >85% (Fig. S1 in the Supporting Material). Fig. 3 shows the RMSD values computed for all intermediate models against the expected open and closed positions, respectively, of their cyclin. To that purpose, each displaced complex along the mode considered was first rotated by RMS structural fitting of the CDK part onto its corresponding target followed by structural fitting of the cyclin part (i.e., displaced structures of CDK2/cyclin A compared to the target x-ray structure of CDK4/cyclin D1, and vice versa, displaced structures of CDK4/cyclin D1 compared to the target x-ray structure of CDK2/cyclin A). The reported RMSD values are those between the cyclins. The reference RMSD value computed between the open and closed conformations of the CDK/cyclin complexes was ~23 Å. For each complex, a linear decrease/increase of RMSD values was observed along mode 7, confirming the importance of this mode in the description of the conformational transition between the open and closed positions of the CDK/cyclin complex. In contrast, minor contributions were observed

Please cite this article in press as: Floquet et al., Conformational Equilibrium of CDK/Cyclin Complexes by Molecular Dynamics with Excited Normal Modes, Biophysical Journal (2015), http://dx.doi.org/10.1016/j.bpj.2015.07.003

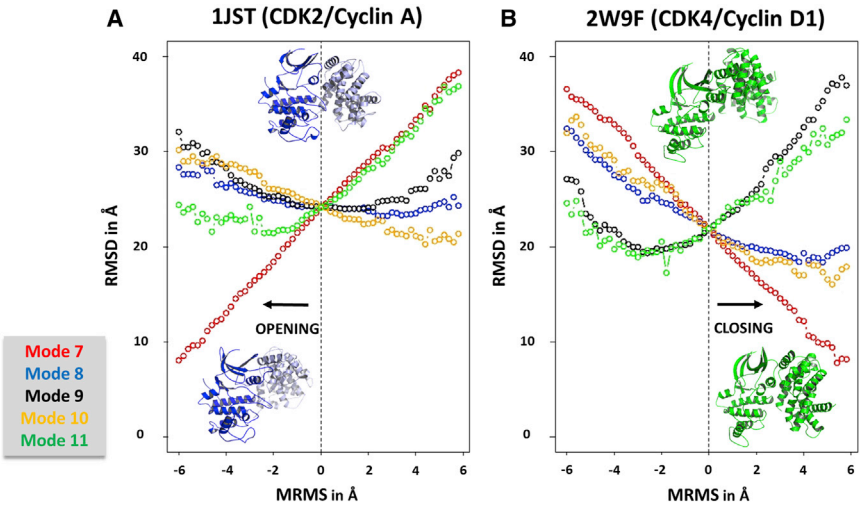

FIGURE 3 RMSD values computed considering the cyclin conformation on the displaced complex along the five lowest-frequency modes and its position in the x-ray target complex after superimposing the respective CDK proteins, as explained in the text. (*A*) Displaced CDK2/cyclin A complex and target CDK4/cyclin D1 complex. (*B*) Displaced CDK4/cyclin D1 complex and target CDK2/cyclin A complex. The MRMS values in the abscissa correspond to the displacements along the modes considered. A MRMS value of 0 corresponds to the initial energy-minimized model used for NM calculations. For purposes of clarity, only the results obtained for the five lowest-frequency NMs of each complex were reported. To see this figure in color, go online.

regarding the subsequent modes (modes 8–11). Moreover, the identification of such intrinsic motion in both complexes strongly suggested the occurrence in solution of relevant, but not yet revealed, conformational states along the mode 7 direction. These states may vary between more open conformations for the CDK2/cyclin A complex and more closed conformations for the CDK4/cyclin D1 than those reported in the related crystallographic structures. Fig. 3 also shows that a very large-amplitude motion, e.g., with an MRMS value >6 Å along mode 7, was required to decrease the global RMSD between the cyclins to a value <7 Å. Indeed, pushing the normal coordinate for the seventh mode further, the linearity of the RMSD variation was lost and reached a plateau before arriving at a nonzero-RMSD structure.

The closed CDK2/cyclin A complex remains closed in water

Using the MDeNM technique (27), we first explored the accessible conformations in explicit solvent obtained upon excitation of mode 7 computed for the CDK2/cyclin A complex. This technique allows coupling between fast and slow motions without the introduction of biases or restraints. Briefly, incremental velocities ($\Delta \boldsymbol{v}^{\mathbf{NM}}$) along the NM directions are added to current velocities obtained after an equilibration MD simulation. This incremental kinetic energy along specific degrees of freedom corresponds to the excitation of one or more low-frequency modes related to large-amplitude motions that are hardly explored during standard MD simulations. Therefore, with multiple short replica MDeNM simulations, large conformational changes are enhanced and the definition of the maximum extent of sampling by mode is solely based on intrinsic features of the system.

Inspection of the MDeNM trajectories revealed that the expected closed/open transition motion was properly explored, even using a moderately low value of incremental temperature (ΔT_{nm}= 5 K). The large-amplitude motion promoted led to a decrease of the RMSD between closed and open states from 23 to 4.2 Å (Fig. S2 *A*). In addition, we noticed the occurrence of more closed conformations, resulting in a marked increase of contact area between CDK2 and cyclin A. The contributions of other modes to the structural transition are not significant, as shown by projections of the concatenated MDeNM trajectory onto them (Fig. S3). To clarify these results, we refer to Movie S1, which shows the sampled conformers in water for CDK2/cyclin A, together with an animation showing the transition between the initial conformation (the equilibrated x-ray structure) and the conformation sharing the lowest RMSD to the open conformation (Fig. S4).

After concatenation of the MDeNM trajectories and clustering of the conformations obtained (using the k-means method), additional 2 ns MD simulations were performed starting from the central conformations (centroids) obtained on each of the 20 resulting clusters. These simulations were required to dissipate the kinetic perturbations previously introduced and to reach a population of conformers in thermodynamic equilibrium (27). Fig. 4 *A* displays the projections of the resulting conformations onto the mode 7 coordinate (*blue line*). The narrow peak centered on 0 Å MRMS indicates a small extent of sampling, and therefore, most of the sampled conformations remained close to the initial structure. Nevertheless, the small peak observed at −2 Å MRMS indicates that open conformations were explored, but to a lesser extent. On the other hand, completely closed conformations (previously suggested by the initial VMOD results in vacuum) were not observed. These results were in striking agreement with the projections of a set of 98 experimental x-ray structures describing the CDK2/cyclin A complex (Fig. 4 *A*, *black line*). Similar results were obtained after a 25 ns standard MD simulation performed in water (Fig. 4 *A*, *red line*), although in this case no open conformations were obtained. Interestingly, a

Please cite this article in press as: Floquet et al., Conformational Equilibrium of CDK/Cyclin Complexes by Molecular Dynamics with Excited Normal Modes, Biophysical Journal (2015), http://dx.doi.org/10.1016/j.bpj.2015.07.003

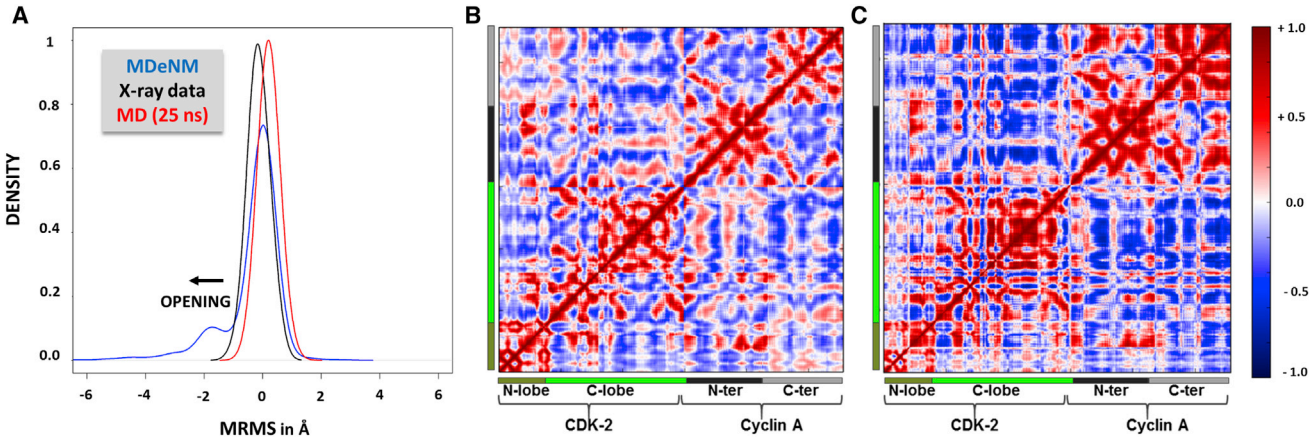

FIGURE 4 (*A*) Results of population analysis based on projections of the conformations obtained for the CDK2/cyclin A complex after MD resampling of the 20 clusters resulting from MDeNM simulations along mode 7 (*blue*), after a screening of the PDB (98 structures) (*black*), and after a 25 ns MD simulation of the starting PDB 1JST structure (*red*). (*B* and *C*) Residue-residue cross-correlation analyses were performed through PCA of the MDeNM data (25 quasimodes) (*B*) or the collected 98 x-ray structures (*C*). The CDK-2 and cyclin A structural domains are highlighted in the margins of each cross-correlation map. The matrices in (*B*) and (*C*) show no significant discrepancies, sharing a Mantel test (40) value of 0.8. To see this figure in color, go online.

comparison of the correlation coefficients between pairs of residues (cross correlations) obtained after PCA of the coordinates obtained from 1) MDeNM simulations (Fig. 4 *B*) or 2) the x-ray data subset (Fig. 4 *C*) confirmed that our MDeNM simulations successfully described the intrinsic collective motions that could be guessed from all available x-ray structures.

To confirm the visual analysis, we performed a Mantel test (40) using R, which yielded a high correlation value (0.8), thus indicating that both cross-correlation maps are indeed similar. Further, a lower correlation value (0.68) was obtained when comparing standard MD and experimental data. This analysis indicates that MDeNM simulations better capture the intrinsic structural variation of the CDK-2/cyclin A complex. Altogether, these results show that the CDK2/cyclin A complex clearly prefers a closed conformation in solution. The same protocol was performed on the CDK2/cyclin A complex after removal of the phosphoryl group on Thr^{160}, but the results were not significantly altered. Among other observations, it was verified that the removal of the phosphoryl group did not affect the overall flexibility of the protein/protein complex or, more specifically, of the activation loop (see Fig. S5).

The open CDK4/cyclin D1 complex can adopt a closed conformation in water

The same protocol was performed on the CDK4/cyclin D1 complex. Results from the MDeNM simulations are reported in Fig. S2 *B*. Again, the opening/closing motion along mode 7 was properly explored during our simulations using a maximum of 5 K excitation, leading to a closed conformation sharing a low 4.4 Å RMSD value against the expected position of the cyclin, and closely related to that observed in the CDK2/cyclin A structure (See Fig. S6). From the analysis of the projections onto the other low-frequency modes, it seems that only mode 9 had a small contribution to closure motions (projections reaching ± 1.5 Å) (Fig. S3). Interestingly, more open conformations were also explored for this complex. The conformations sampled during MDeNM simulations are reported in Movie S2. After clustering of the excited trajectories and resampling of representative conformations during MD simulations along this motion, we obtained the equilibrium populations (Fig. 5, *blue line*). As compared to CDK2/cyclin A, larger conformational changes were observed for this complex, with significant sampling of closed conformations at 4 Å MRMS. Open conformations beyond the crystallographic structure were also observed. Although for CDK4 the amount of x-ray data is limited, our results suggest that a closed conformation of the CDK4/cyclin D1 complex, closely related to that captured experimentally for the CDK2/cyclin A, could be generated. Similar results were obtained starting from the CDK4/cyclin D3 complex, suggesting a common feature that does not depend on the cyclin partner (data not shown). The equilibrium populations obtained from a standard MD simulation (Fig. 5, *red line*) showed limited sampling along the opening/closing motion, reinforcing the importance of MDeNM in the exploration of large structural transitions.

Conformational propensities on CDK/cyclin complexes are related to their distinct networks of frustrated contacts

We asked whether the distinct conformational propensities observed in the MDeNM simulations of CDK/cyclin complexes could be associated with their distinct networks of contacts. In this context, we performed a frustration

Please cite this article in press as: Floquet et al., Conformational Equilibrium of CDK/Cyclin Complexes by Molecular Dynamics with Excited Normal Modes, Biophysical Journal (2015), http://dx.doi.org/10.1016/j.bpj.2015.07.003

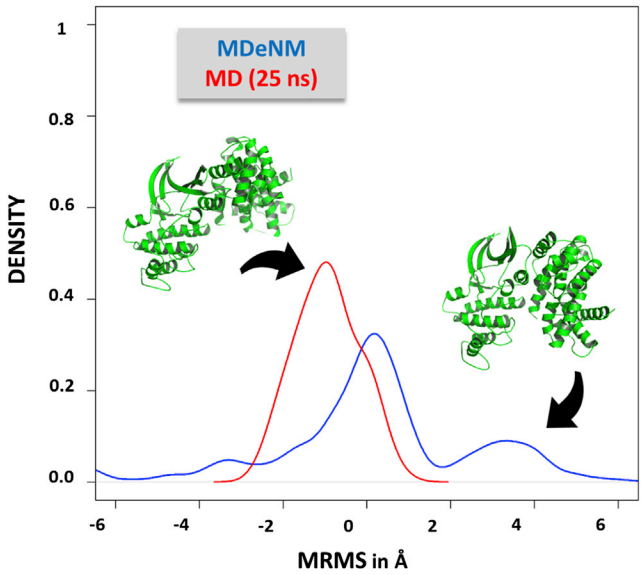

FIGURE 5 Results of population analysis based on projections of the conformations obtained for the CDK4/cyclin D1 complex after MD resampling of the 20 clusters resulting from MDeNM simulations along mode 7 (*blue*) and after a 25 ns MD simulation of the starting PDB 2W9F structure (*red*). To see this figure in color, go online.

analysis (39) on both complexes considering their open and closed forms. Briefly, this analysis allows one to determine how localized sequence and conformational perturbations influence energetic frustrations, measuring how favorable a particular contact is relative to other possible local interactions. Comparing the closed and open conformations of each complex, the number of highly frustrated contacts is higher in the CDK-2/cyclin A open state. In contrast, the CDK-4/cyclin D1 closed state is more frustrated. The decrease of highly frustrated interactions per residue (Fig. 6, *C* and *D*, *red*) when going from an open to a closed state (*negative values*) in CDK2/cyclin A, but not in CDK4/cyclin D1, corroborates the increased propensity of the former to remain in a closed state, whereas the latter is more stable in an open state. The opposite trend observed regarding the number of minimally frustrated contacts reinforces this observation (Fig. 6, *C* and *D*). Fig. 6, *A* and *B*, display how the local energetic frustration is distributed over the less-frustrated state of each CDK/cyclin complex. It is interesting to note that they correspond to their available crystallographic structures.

However, it is noticeable that even the most favorable state of each complex displays localized frustrations, as shown in Fig. 6, *A* and *B*. Both networks show that individual domains are connected by several minimally frustrated contacts, whereas highly frustrated regions are mostly localized at the interface. As previously mentioned (39), these frustrated contacts are associated with regions prone to undergoing conformational changes, which also corroborates the occurrence of large-amplitude motions in these complexes.

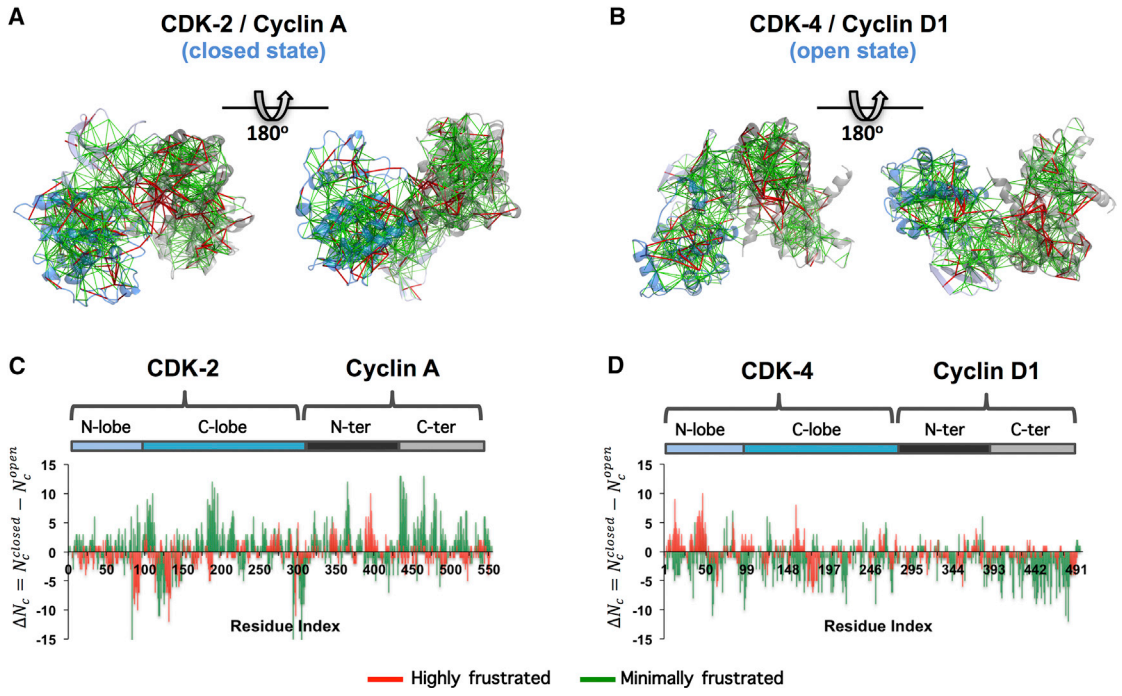

FIGURE 6 Localizing and evaluating frustration in CDK/cyclin complexes. Minimally and highly frustrated contacts are represented in green and red, respectively. (*A* and *B*) Visualization of the frustration networks for the less-frustrated state of each complex. (*C* and *D*) Variation of the number of frustrated contacts upon structural transition from an open to a closed conformation ($\Delta N_c = N_c^{closed} - N_c^{open}$). The domain definitions of each complex are given in the top part of each plot. To see this figure in color, go online.

Please cite this article in press as: Floquet et al., Conformational Equilibrium of CDK/Cyclin Complexes by Molecular Dynamics with Excited Normal Modes, Biophysical Journal (2015), http://dx.doi.org/10.1016/j.bpj.2015.07.003

Role of the T-loop conformation in the opening/closing motion of CDK/cyclin complexes

In the starting structure of the CDK4/cyclin D1 complex (PDB 2W9F), the T-loop is found in an inactive conformation (see Fig. 1). To investigate the putative role of this loop conformation in the open/closed equilibrium, we built a hybrid model based on the starting structure but with the T-loop changed to an active conformation (as observed in the CDK2/cyclin A complex). After equilibration of this model with CHARMM, the computed mode 7 again described the open/closed transition, presenting a contribution to the overall fluctuations similar to that observed for the original CDK-4/cyclin D1 complex (Fig. S1). Analysis of MDeNM simulations yielded similar results to those observed for the inactive loop complex, showing a greater flexibility of the cyclin than was displayed by the CDK2/cyclin A complex (data not shown). After clustering and resampling of intermediate conformations, as performed for the other complexes, the thermodynamic equilibrium populations reported in Fig. 7 were obtained. Compared to the 2W9F complex, we observed both open and closed states in similar proportions, a clear modification of the profile previously obtained with simulations starting with an inactive loop conformation.

Dynamical cross-correlation analyses of CDK2/cyclin A and CDK4/cyclin D1 complexes

The comparison between the dynamical correlation patterns observed in the complexes revealed some important differences. Fig. 8 shows the cross correlations calculated after MD sampling from excited clustered structures. The corresponding two-dimensional maps are given in Figs. 4 *B* (CDK2/cyclin A) and S7 (CDK-4/cyclin D1 and the hybrid model). In both complexes, positive correlations were observed within the C-terminal portions of both CDK and cyclin. However, the N-terminal domains of both CDK4 and cyclin D1 presented stronger correlations than did those of the CDK2/cyclin A complex (Figs. 4 *B* and S7). The differences in the anticorrelation patterns were striking. Whereas in the CDK2 /cyclin A complex the anticorrelations were noticed only between a small part of the C-lobe and the C-terminal of cyclin A, in CDK4/cyclin D1, both intra- and intermolecular anti-correlations were observed. This finding interestingly demonstrated that the opening/closing motion that was much more explored in the CDK4/cyclin D1 complex was coupled to an intrinsic dynamics of the kinase, moving its two lobes toward opposite directions. The PSTAIRE helix at the interface of the two proteins clearly plays a key role in the mechanical transmission. Interestingly, when the T-loop conformation was switched (hybrid complex), both inter- and intramolecular anticorrelations were weakened, resulting in an intermediate profile between CDK4 (2W9F) and CDK2 complexes, definitively demonstrating the role of this motion in the transmission of mechanical information between the cyclin and kinase partners.

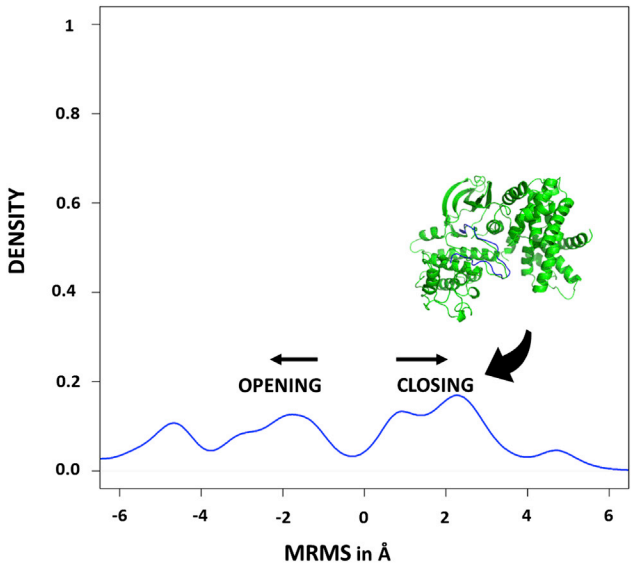

FIGURE 7 Equilibrium population distribution obtained after projections onto mode 7 of the conformations explored by MD after MDeNM simulations of the HYBRID model. To see this figure in color, go online.

DISCUSSION

In this study, we explored the large-amplitude motions occurring in two CDK/cyclin complexes, 1) CDK2/cyclin A, whose x-ray structure corresponds to a closed state of the heterodimeric complex, and 2) CDK4/cyclin D1, which has been elucidated in an open state. The closed and open states are defined by the relative position of the cyclin with respect to the CDK subunit. In both cases, the lowest-frequency NM described the conformational transition between the closed and open states, suggesting that such motion is an intrinsic propensity of both CDK/cyclin complexes.

As calculations were performed in vacuum, they did not account for solvent effects, which ultimately impair a proper estimation of amplitudes of motion and the populations of the different conformational states in thermodynamic equilibrium at 300 K. To gain further insight into these issues, the lowest-frequency mode calculated for each of the complexes was assigned as a privileged direction in MDeNM simulations, where collective motions are kinetically excited within MD simulations. The MDeNM simulations allowed us to generate a large set of intermediate excited structures along the transition pathway described by the lowest mode in either of the two complexes studied. The results clearly showed that such motion is energetically feasible in both complexes.

Further, from the projections of the trajectories onto mode 7, we noticed energetically accessible conformations along

Please cite this article in press as: Floquet et al., Conformational Equilibrium of CDK/Cyclin Complexes by Molecular Dynamics with Excited Normal Modes, Biophysical Journal (2015), http://dx.doi.org/10.1016/j.bpj.2015.07.003

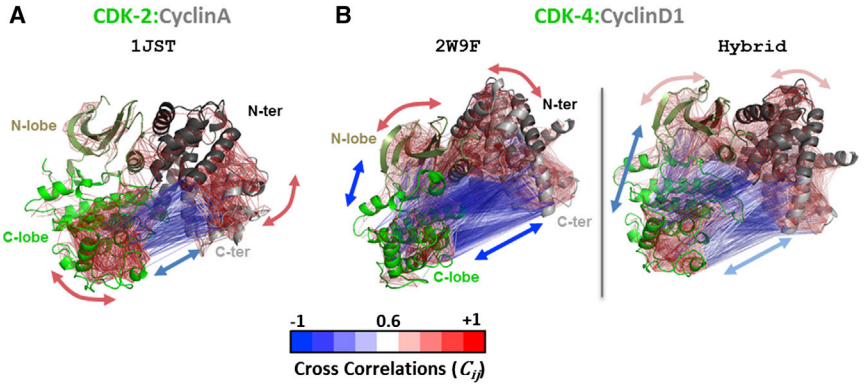

FIGURE 8 Dynamical cross correlations ($C_{(i,j)}$) plotted onto the structures of CDK/cyclin complexes CDK2/cyclin A (*A*) and CDK4/cyclin D1 (*B*). The red and blue edges connect pairs of residues that are correlated or anticorrelated, respectively. Darker edges indicate stronger couplings, as reported in the color scale. The most important domains were highlighted and the arrows in the margins of the structures indicate the main directions of large-amplitude motions observed during the trajectories. To see this figure in color, go online.

this collective coordinate beyond those found in the crystal structures. To obtain populations of structures in thermodynamic equilibrium, a set of unrestrained MD simulations was carried out starting from representative structures retrieved after a clustering procedure on the MDeNM trajectories. For the CDK2/cyclin A complex, we observed that most of the sampled conformations were predominantly closed, therefore resembling the distribution obtained from a set of 98 crystallographic structures. In contrast, CDK4/cyclin D1 presented a much greater conformational plasticity, with both closed and open states markedly populated, although the crystal structure of this complex only reveals the existence of an open conformation. This feature was in agreement with the higher tendency of this complex to be refractory to structure determination.

We also identified the distinct networks of frustrated contacts in full accordance with the structural and dynamic data, since the CDK-2/cyclin A open state and the CDK-4/cyclin D1 closed state are more frustrated, being probably less stable in solution.

It is important to emphasize the importance of such hybrid calculations combining NMA and MD on the evaluation of dynamical features of complexes in a complete aqueous environment. Standard MD used alone usually fails to properly account for such large conformational changes, especially when opening/closing mechanisms are involved. Although NMA yields propensities for such transitions, the equilibrium populations only can be disclosed when the large-amplitude motions are evaluated in the context of a dynamical simulation (27).

From the conformational equilibrium, several dynamical properties can be obtained and compared to experimental data with significant agreement, as shown here (see Fig. 4), as well as for other systems (27). In some applications, MDeNM was shown to perform better than other well-established enhanced sampling methods such as metadynamics or umbrella sampling (27,41–46).

We also propose an important role of the T-loop conformation on the equilibrium between open and closed states. Nevertheless, modifying only its conformation was not sufficient to fully switch the intrinsic dynamical profile of CDK4/cyclin D1 to that observed for CDK2/cyclin A. The effect of loop conformations within the overall dynamics on proteins or complexes is of general interest. We recently showed the importance of the catalytic loop conformation in the context of opening/closing events taking place on the glutamate decarboxylase protein (47). We anticipate that this conformational flexibility may enable such complexes to adapt their conformation upon interaction with other partners, or may occur and be prompted upon substrate binding to achieve optimal phosphoryl transfer reaction. It has indeed been suggested that the interaction of CDK4/cyclin D substrate, p107Rb, may bring CDK4 and cyclin D closer together so as to promote the conformational changes necessary to bring the CDK4 T-loop into an active conformation (18,19). Our results reveal that this conformational change is indeed energetically possible and permitted to generate conformational ensembles that will now be useful for the design of drugs targeting the CDK/cyclin interface (see Fig. S8). These studies are also in line with the fact that CDK4, being a central portal for integration of cell growth and inhibition signals to stimulate exit from quiescence and entry into the cycle of cell growth and division, may also bind to other cyclins.

SUPPORTING MATERIAL

List of the experimental structures considered for ensemble calculations, eight figures, and two movies are available at http://www.biophysj.org/biophysj/supplemental/S0006-3495(15)00674-8.

AUTHOR CONTRIBUTIONS

N.F. proposed the subject, designed the research, carried out the calculations, analyzed the results, and wrote the article; M.G.S.C. contributed analytic tools, analyzed the results, and wrote the article; P.R.B. introduced the necessary improvements in the analysis of results and helped with writing the article; P.R. contributed to methodological development; P.M.B. contributed to methodological improvements; F.R. helped in running the calculations; J.M. helped in the writing; M.C.M. proposed the subject and wrote the article; and D.P. designed the research, analyzed data, and wrote the article.

Please cite this article in press as: Floquet et al., Conformational Equilibrium of CDK/Cyclin Complexes by Molecular Dynamics with Excited Normal Modes, Biophysical Journal (2015), http://dx.doi.org/10.1016/j.bpj.2015.07.003

ACKNOWLEDGMENTS

M.G.S.C, P.R.B., P.R., P.M.B., and D.P. thank the Brazilian-French collaboration project Coordenação de Aperfeiçoamento de Pessoal de Nível Superior/Comité Français d'Evaluation de la Coopération Scientifique et Universitaire avec le Brésil.

REFERENCES

1. Morgan, D. O. 1997. Cyclin-dependent kinases: engines, clocks, and microprocessors. *Annu. Rev. Cell Dev. Biol.* 13:261–291.
2. Satyanarayana, A., and P. Kaldis. 2009. Mammalian cell-cycle regulation: several Cdks, numerous cyclins and diverse compensatory mechanisms. *Oncogene.* 28:2925–2939.
3. Malumbres, M., and M. Barbacid. 2005. Mammalian cyclin-dependent kinases. *Trends Biochem. Sci.* 30:630–641.
4. Obaya, A. J., and J. M. Sedivy. 2002. Regulation of cyclin-Cdk activity in mammalian cells. *Cell. Mol. Life Sci.* 59:126–142.
5. Lim, S., and P. Kaldis. 2013. Cdks, cyclins and CKIs: roles beyond cell cycle regulation. *Development.* 140:3079–3093.
6. Malumbres, M., and M. Barbacid. 2009. Cell cycle, CDKs and cancer: a changing paradigm. *Nat. Rev. Cancer.* 9:153–166.
7. Lapenna, S., and A. Giordano. 2009. Cell cycle kinases as therapeutic targets for cancer. *Nat. Rev. Drug Discov.* 8:547–566.
8. Bruyère, C., and L. Meijer. 2013. Targeting cyclin-dependent kinases in anti-neoplastic therapy. *Curr. Opin. Cell Biol.* 25:772–779.
9. Peyressatre, M., C. Prével, …, M. C. Morris. 2015. Targeting cyclin-dependent kinases in human cancers: from small molecules to peptide inhibitors. *Cancers (Basel).* 7:179–237.
10. Lolli, G. 2010. Structural dissection of cyclin dependent kinases regulation and protein recognition properties. *Cell Cycle.* 9:1551–1561.
11. Schulman, B. A., D. L. Lindstrom, and E. Harlow. 1998. Substrate recruitment to cyclin-dependent kinase 2 by a multipurpose docking site on cyclin A. *Proc. Natl. Acad. Sci. USA.* 95:10453–10458.
12. Coleman, T. R., and W. G. Dunphy. 1994. Cdc2 regulatory factors. *Curr. Opin. Cell Biol.* 6:877–882.
13. Brown, N. R., M. E. Noble, …, J. A. Endicott. 1999. Effects of phosphorylation of threonine 160 on cyclin-dependent kinase 2 structure and activity. *J. Biol. Chem.* 274:8746–8756.
14. Jeffrey, P. D., A. A. Russo, …, N. P. Pavletich. 1995. Mechanism of CDK activation revealed by the structure of a cyclinA-CDK2 complex. *Nature.* 376:313–320.
15. Morris, M. C., C. Gondeau, …, G. Divita. 2002. Kinetic mechanism of activation of the Cdk2/cyclin A complex. Key role of the C-lobe of the Cdk. *J. Biol. Chem.* 277:23847–23853.
16. Hagopian, J. C., M. P. Kirtley, …, J. Lew. 2001. Kinetic basis for activation of CDK2/cyclin A by phosphorylation. *J. Biol. Chem.* 276:275–280.
17. Russo, A. A., P. D. Jeffrey, and N. P. Pavletich. 1996. Structural basis of cyclin-dependent kinase activation by phosphorylation. *Nat. Struct. Biol.* 3:696–700.
18. Day, P. J., A. Cleasby, …, H. Jhoti. 2009. Crystal structure of human CDK4 in complex with a D-type cyclin. *Proc. Natl. Acad. Sci. USA.* 106:4166–4170.
19. Takaki, T., A. Echalier, …, M. E. M. Noble. 2009. The structure of CDK4/cyclin D3 has implications for models of CDK activation. *Proc. Natl. Acad. Sci. USA.* 106:4171–4176.
20. Jeffrey, P. D., L. Tong, and N. P. Pavletich. 2000. Structural basis of inhibition of CDK-cyclin complexes by INK4 inhibitors. *Genes Dev.* 14:3115–3125.
21. Baumli, S., G. Lolli, …, L. N. Johnson. 2008. The structure of P-TEFb (CDK9/cyclin T1), its complex with flavopiridol and regulation by phosphorylation. *EMBO J.* 27:1907–1918.
22. Barrett, C. P., and M. E. M. Noble. 2005. Molecular motions of human cyclin-dependent kinase 2. *J. Biol. Chem.* 280:13993–14005.
23. Bahar, I., T. R. Lezon, …, E. Eyal. 2010. Global dynamics of proteins: bridging between structure and function. *Annu. Rev. Biophys.* 39:23–42.
24. Floquet, N., P. Durand, …, D. Perahia. 2009. Collective motions in glucosamine-6-phosphate synthase: influence of ligand binding and role in ammonia channelling and opening of the fructose-6-phosphate binding site. *J. Mol. Biol.* 385:653–664.
25. Floquet, N., C. M'Kadmi, …, J. Martinez. 2010. Activation of the ghrelin receptor is described by a privileged collective motion: a model for constitutive and agonist-induced activation of a sub-class A G-protein coupled receptor (GPCR). *J. Mol. Biol.* 395:769–784.
26. Louet, M., D. Perahia, …, N. Floquet. 2011. A concerted mechanism for opening the GDP binding pocket and release of the nucleotide in hetero-trimeric G-proteins. *J. Mol. Biol.* 411:298–312.
27. Costa, M. G. S., P. R. Batista, …, D. Perahia. 2015. Exploring free energy landscapes of large conformational changes: molecular dynamics with excited normal modes. *J. Chem. Theory Comput.* 11:2755–2767.
28. Damian, M., S. Mary, …, J.-L. Banères. 2015. Ghrelin receptor conformational dynamics regulate the transition from a preassembled to an active receptor:Gq complex. *Proc. Natl. Acad. Sci. USA.* 112:1601–1606.
29. Webb, B., and A. Sali. 2014. Comparative protein structure modeling using MODELLER. *Curr. Protoc. Protein Sci.* Chapter 2: Unit 2.9.
30. Brooks, B. R., C. L. Brooks, 3rd, …, M. Karplus. 2009. CHARMM: the biomolecular simulation program. *J. Comput. Chem.* 30:1545–1614.
31. Jo, S., T. Kim, …, W. Im. 2008. CHARMM-GUI: a web-based graphical user interface for CHARMM. *J. Comput. Chem.* 29:1859–1865.
32. Perahia, D., and L. Mouawad. 1995. Computation of low-frequency normal modes in macromolecules: improvements to the method of diagonalization in a mixed basis and application to hemoglobin. *Comput. Chem.* 19:241–246.
33. Koukos, P. I., and N. M. Glykos. 2013. Grcarma: a fully automated task-oriented interface for the analysis of molecular dynamics trajectories. *J. Comput. Chem.* 34:2310–2312.
34. Phillips, J. C., R. Braun, …, K. Schulten. 2005. Scalable molecular dynamics with NAMD. *J. Comput. Chem.* 26:1781–1802.
35. Bakan, A., L. M. Meireles, and I. Bahar. 2011. ProDy: protein dynamics inferred from theory and experiments. *Bioinformatics.* 27:1575–1577.
36. Bakan, A., and I. Bahar. 2009. The intrinsic dynamics of enzymes plays a dominant role in determining the structural changes induced upon inhibitor binding. *Proc. Natl. Acad. Sci. USA.* 106:14349–14354.
37. Grant, B. J., A. P. C. Rodrigues, …, L. S. D. Caves. 2006. Bio3d: an R package for the comparative analysis of protein structures. *Bioinformatics.* 22:2695–2696.
38. Jenik, M., R. G. Parra, …, D. U. Ferreiro. 2012. Protein frustratometer: a tool to localize energetic frustration in protein molecules. *Nucleic Acids Res.* 40:W348–W351.
39. Ferreiro, D. U., J. A. Hegler, …, P. G. Wolynes. 2007. Localizing frustration in native proteins and protein assemblies. *Proc. Natl. Acad. Sci. USA.* 104:19819–19824.
40. Mantel, N. 1967. The detection of disease clustering and a generalized regression approach. *Cancer Res.* 27:209–220.
41. Spiwok, V., P. Lipovová, and B. Králová. 2007. Metadynamics in essential coordinates: free energy simulation of conformational changes. *J. Phys. Chem. B.* 111:3073–3076.
42. Spiwok, V., Z. Šućur, and P. Hošek. 2014. Enhanced sampling techniques in biomolecular simulations. *Biotechnol. Adv.* Published online December 5: 2014. http://dx.doi.org/10.1016/j.biotechadv.2014.11.011.
43. Ho, B. K., D. Perahia, and A. M. Buckle. 2012. Hybrid approaches to molecular simulation. *Curr. Opin. Struct. Biol.* 22:386–393.

44. Batista, P. R., G. Pandey, …, C. H. Robert. 2011. Free energy profiles along consensus normal modes provide insight into HIV-1 protease flap opening. *J. Chem. Theory Comput.* 7:2348–2352.

45. Wang, J., Q. Shao, …, W. Zhu. 2014. Exploring transition pathway and free-energy profile of large-scale protein conformational change by combining normal mode analysis and umbrella sampling molecular dynamics. *J. Phys. Chem. B.* 118:134–143.

46. Sun, H., S. Tian, …, T. Hou. 2015. Revealing the favorable dissociation pathway of type II kinase inhibitors via enhanced sampling simulations and two-end-state calculations. *Sci. Rep.* 5:8457.

47. Kass, I., D. E. Hoke, …, A. M. Buckle. 2014. Cofactor-dependent conformational heterogeneity of GAD65 and its role in autoimmunity and neurotransmitter homeostasis. *Proc. Natl. Acad. Sci. USA.* 111:E2524–E2529.

Biophysical Journal

Supporting Material

Conformational Equilibrium of CDK/Cyclin Complexes by Molecular Dynamics with Excited Normal Modes

Nicolas Floquet,[1,*] Mauricio G. S. Costa,[2] Paulo R. Batista,[2] Pedro Renault,[3] Paulo M. Bisch,[3] Florent Raussin,[1] Jean Martinez,[1] May C. Morris,[1] and David Perahia[4,*]

[1]Institut des Biomolécules Max Mousseron (IBMM), Centre National de la Recherche Scientifique UMR 5247, Université de Montpellier, Ecole Normale Supérieure de Chimie de Montpellier, Faculté de Pharmacie, Montpellier, France; [2]Programa de Computação Científica, Fundação Oswaldo Cruz, Rio de Janeiro, Brazil; [3]Instituto de Biofísica Carlos Chagas Filho, Universidade Federal do Rio de Janeiro, Rio de Janeiro, Brazil; and [4]Laboratoire de Biologie et de Pharmacologie Appliquée, Ecole Normale Supérieure de Cachan, Centre National de la Recherche Scientifique, Cachan, France

List of experimental structures considered for the calculations of structural variations with Prody:

2BKZ 1OKW 1OKV 1H1R 2C6T 2WXV 1VYW 3EOC 1OL1
1OL2 2WEV 4I3Z 1QMZ 3MY5 4EOI 4EOJ 4EOK 4EOL
4EOM 4EON 4EOO 1H28 1H25 1H24 4EOR 4EOS 3TNW
2X1N 4BCM 4BCK 2WIP 2WIH 4BCQ 4BCP 2C5X 2C5V
2C5N 2C5O 1URC 4EOP 1H27 1H26 1H1P 1H1Q 1H1S
1JST 1JSU 2WMB 2WMA 2UZL 2UZD 2UZB 4EOQ 2I40
2WHB 3DDQ 3DDP 2CCH 2CCI 1OIU 1OIY 2UZE 1OI9
2CJM 3BHV 3BHU 3BHT 2C4G 1PKD 1OGU 4CFM 2V22
2WPA 4CFU 4CFW 4CFV 4CFX 2WFY 4CFN 1FVV 2IW9
2IW8 2IW6 1E9H 1FIN 3QHW 3QHR 3F5X 4II5 2G9X
3DOG 1P5E 3EID 3EJ1 2UUE 1GY3 2BPM 4FX3

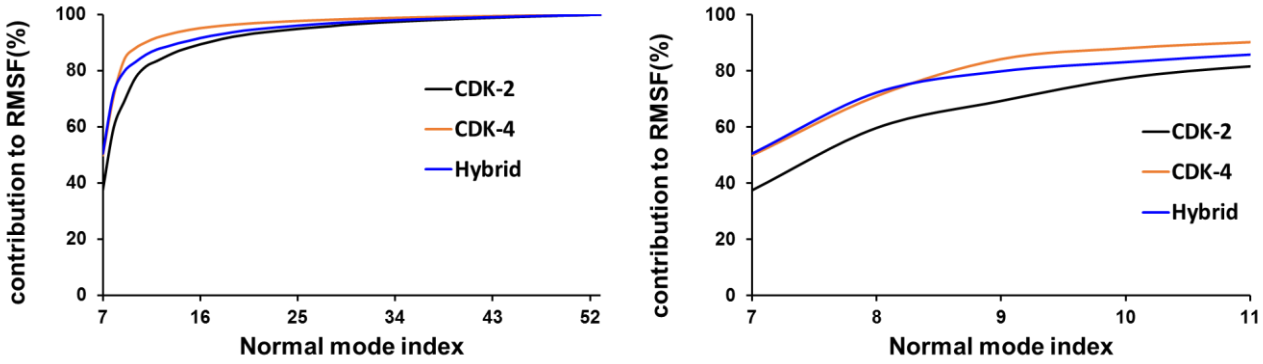

Figure S1: cumulative contribution of each low frequency NM to the overall fluctuations of the three CDK2, CDK4 and Hybrid complexes; left figure from modes 7 to 52, and right figure from modes 7 to 11 for more clarity.

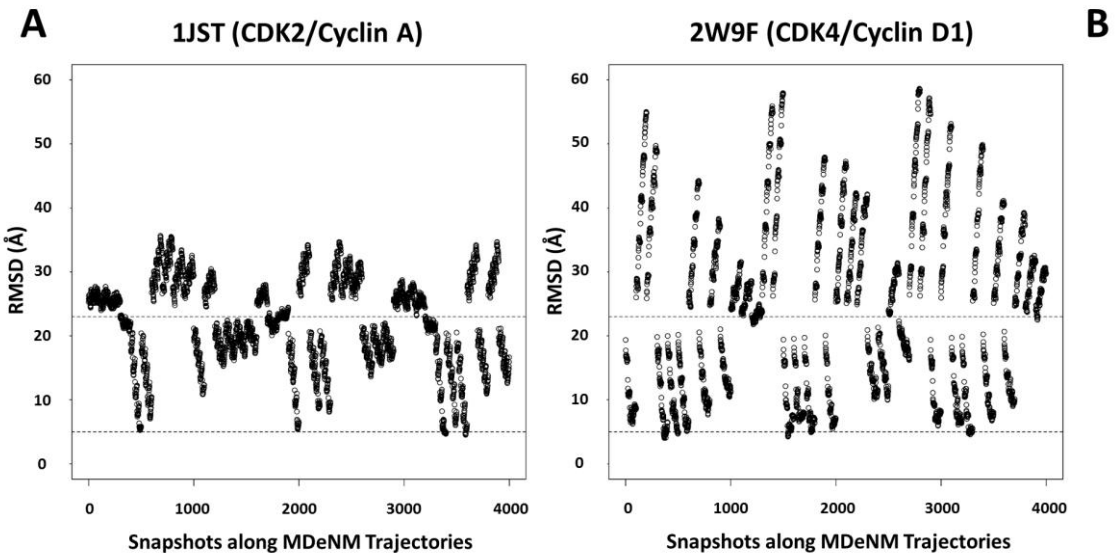

Figure S2: RMSD values computed along MDeNM trajectories and against the open (A) and the closed (B) positions of the Cyclin in the CDK2/Cyclin A (A) and in the CDK4/Cyclin D1 (B) complexes.

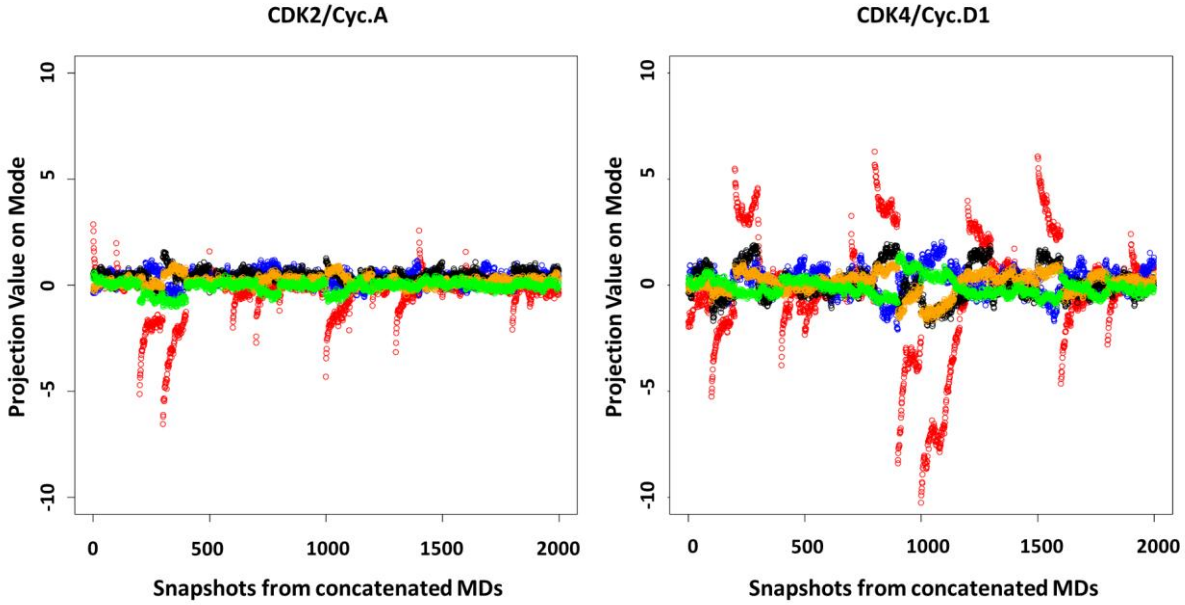

Figure S3: Contributions of modes 7 to 11 (red, blue, black, orange, green in the respective order) to the open/closed conformational transition of the two CDK2/Cyc.A and CDK4/Cyc.D1 complexes.

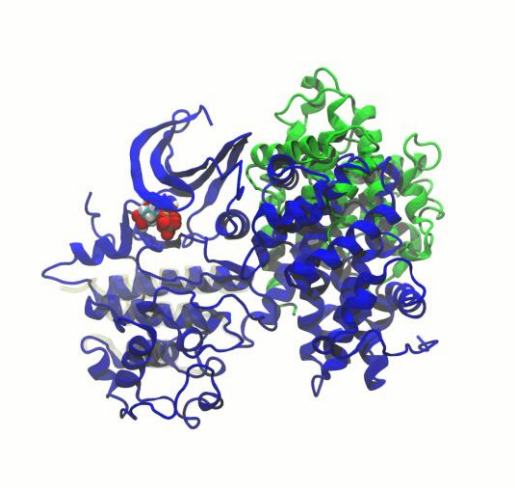

Figure S4: Animated gif picture showing, after MDeNM simulations of the 1JST structure, the transition between the starting equilibrated conformation and that sharing the lowest RMSD value against the « open » position of the Cyclin partner. The three α-helices of the Kinase used for structural fit purpose were highlighted in yellow.

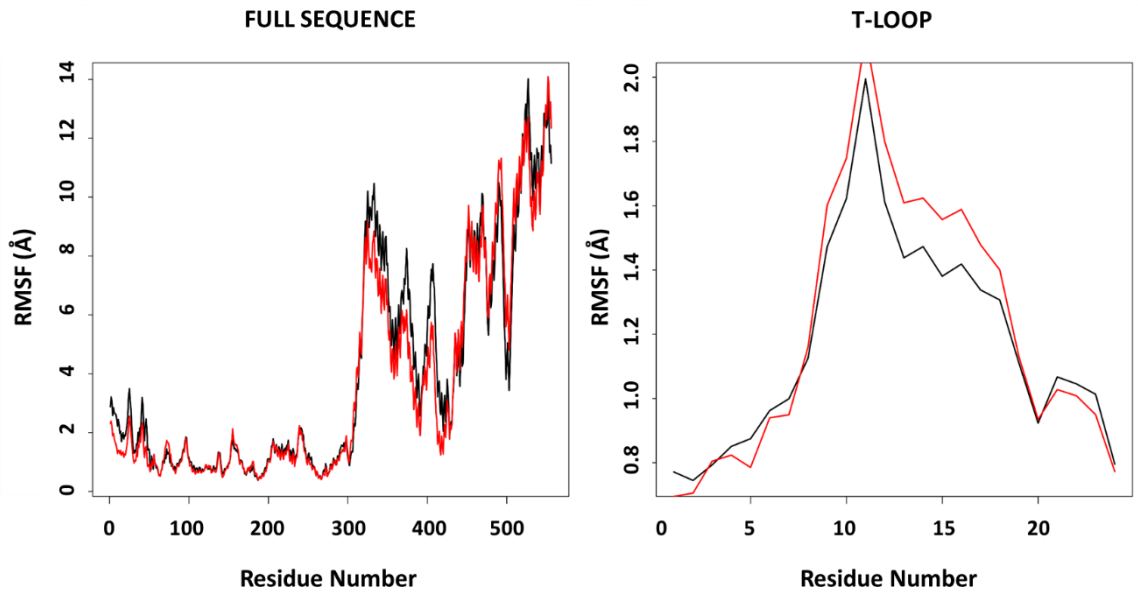

Figure S5: Per-residue RMSFs computed for the concatenated trajectories starting from each centroid obtained after clustering. Black and red lines correspond to simulations with or without the phosphate group on THR160.

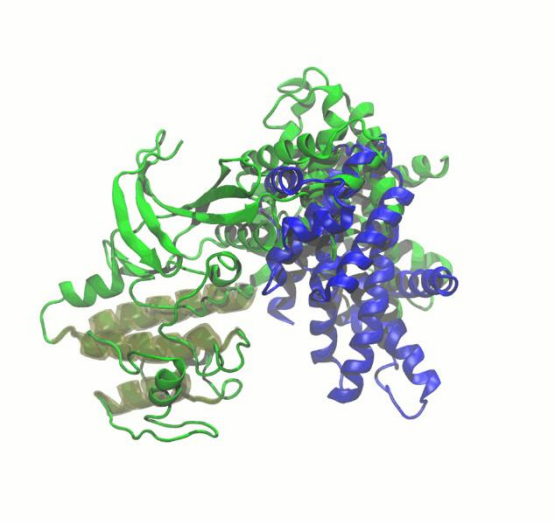

Figure S6: Animated gif picture showing, after MDeNM simulations of the 2W9F structure, the transition between the starting equilibrated conformation and that sharing the lowest RMSD value against the « closed » position of the Cyclin partner. The three α-helices of the Kinase used for structural fit purpose were highlighted in yellow.

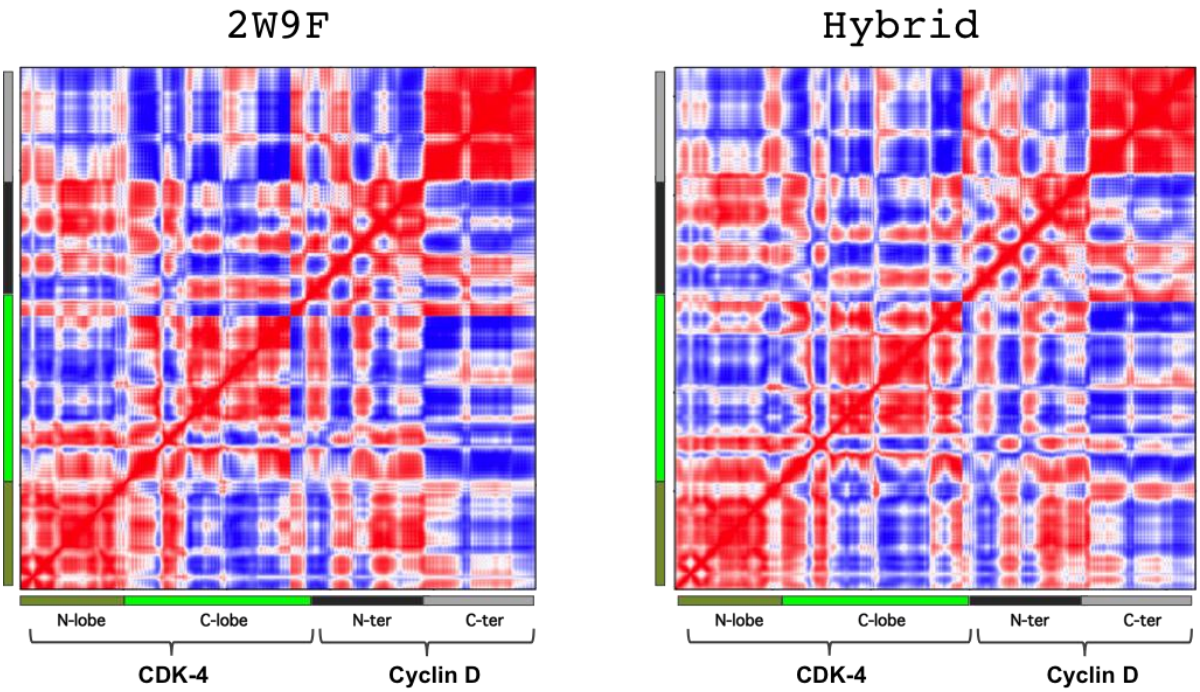

Figure S7: Residue-Residue cross-correlations analyses for the CDK4/Cyclin D1 complex (2W9F: left); and for the Hybrid complex (right). The corresponding structural domains are highlighted in the margins of each cross correlation map.

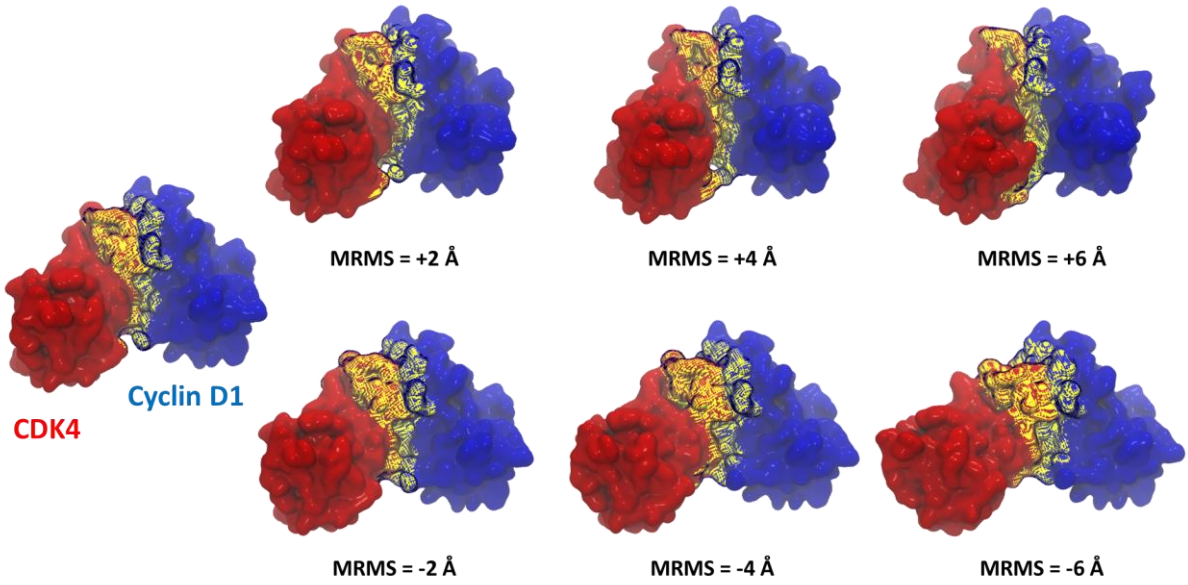

Figure S8 : Evolution of the CDK4:Cyclin D1 surface of interaction (reported in yellow) along the Mode 7 computed for this complex. This shows the interest in using these different models for docking experiments.

Movie 1: MDeNM results obtained for the CDK2/Cyclin A complex. The "open" position of Cyclin A that was extrapolated from the CDK4/Cyclin D1 complex was reported in green.

Movie 2: MDeNM results obtained for the CDK4/Cyclin D1 complex. The position of Cyclin D1 that was extrapolated from the CDK2/Cyclin A complex was reported in blue.